A New Approach to Synthesis of Periodic Mesoporous Organosilicas: Taking Advantage of Self-Assembly and Reactivity of Organic Precursors

Shihai Gu and Mietek Jaroniec*

Department of Chemistry, Kent State University, Kent, Ohio, 44242, USA
E-mail: jaroniec@kent.edu

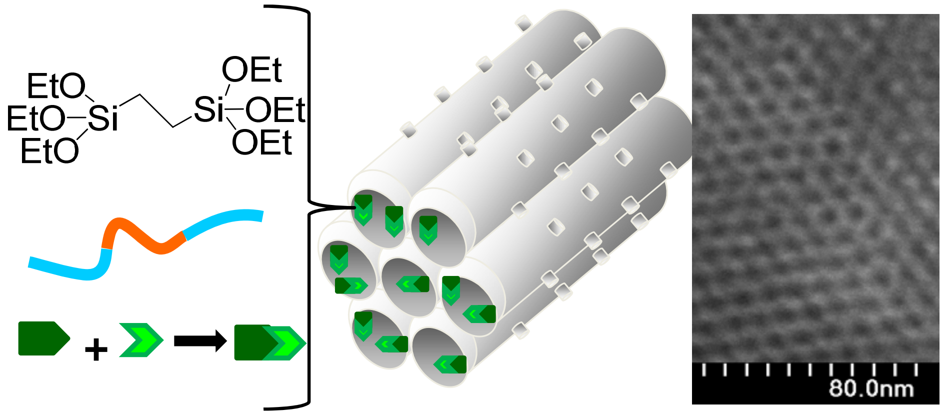

self-assembly & chemical reactions

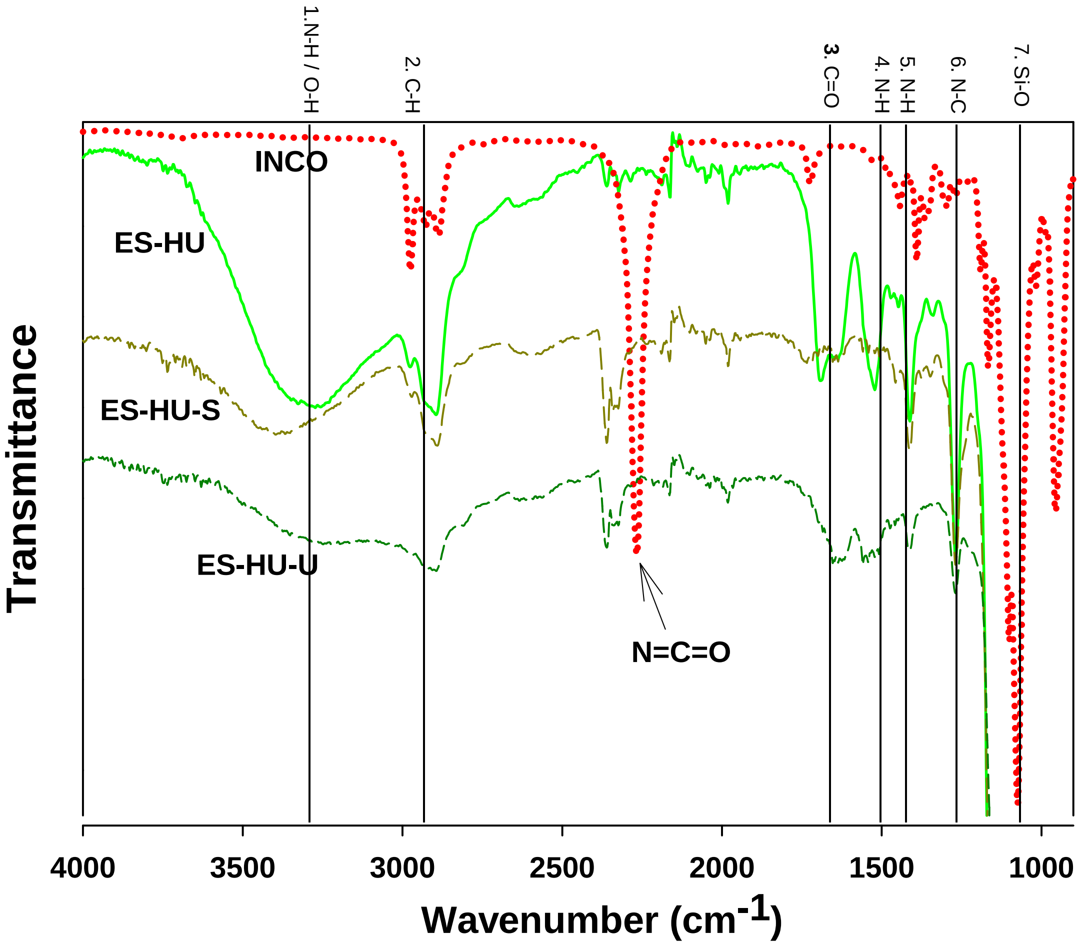

Figure S1. IR spectra of the multifunctional PMO samples (ES-HU, ES-HU-S and ES-HU-U) with N-hydroxyurea functionality (formed via reaction of isocyanate and hydroxylamine HCl salt) in comparison to the spectrum of 3-isocyanatopropyltriethoxysilane precursor. The broad peaks (1) between 3000 and 3500 cm^{-1} can be attributed to N-H stretch and O-H stretch, the peaks (2) around 2900 to 3000 cm^{-1} can be assigned to C-H stretch, the peaks (3) around 1650 cm^{-1} can be mainly attributed to C=O stretch, the peaks (4 & 5) around 1500 cm^{-1} can be caused by N-H stretch and amide II bands, the peaks (6) around 1300 cm^{-1} can be attributed to C-N stretch, and the high intensity peaks (7) below 1110 cm^{-1} are mainly related to Si-O in the ethane-silica framework. Also, there are unmarked peaks around 2300 cm^{-1}, which could be caused by hydroxyurea isomer C=N or unreacted C=N=O.

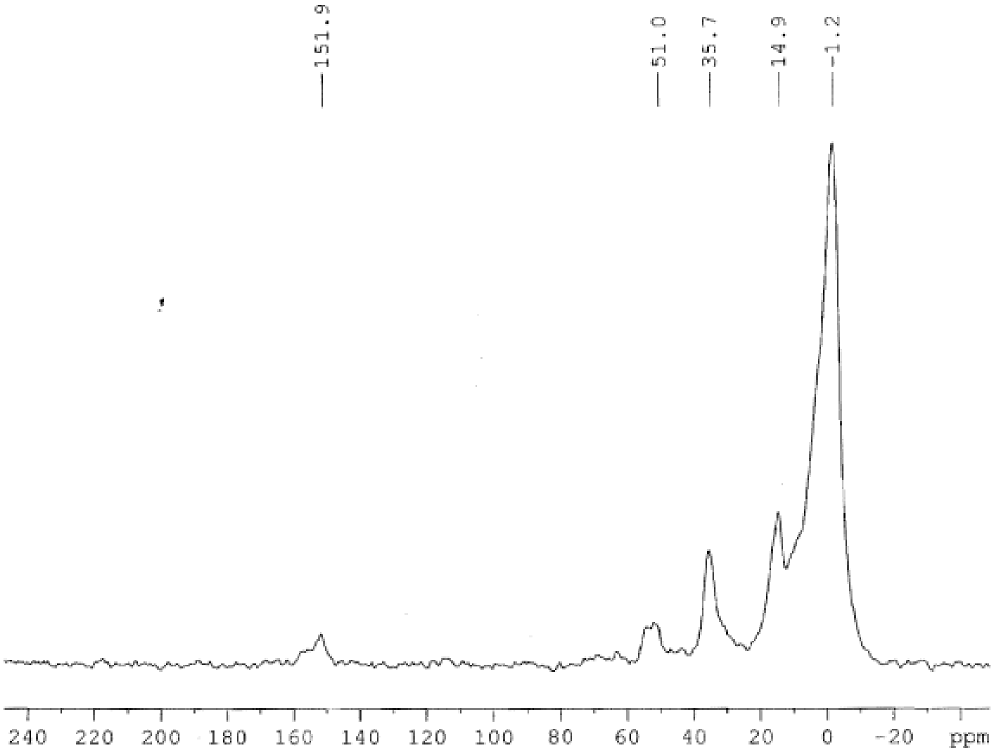

Figure S2. Solid state ^{13}C-NMR of the ES-HU PMO sample obtained by one pot synthesis without acid catalyst showing a peak at 151.9 ppm, which confirms the presence of carbonyl-type carbon in the pendant N-hydroxyurea group.

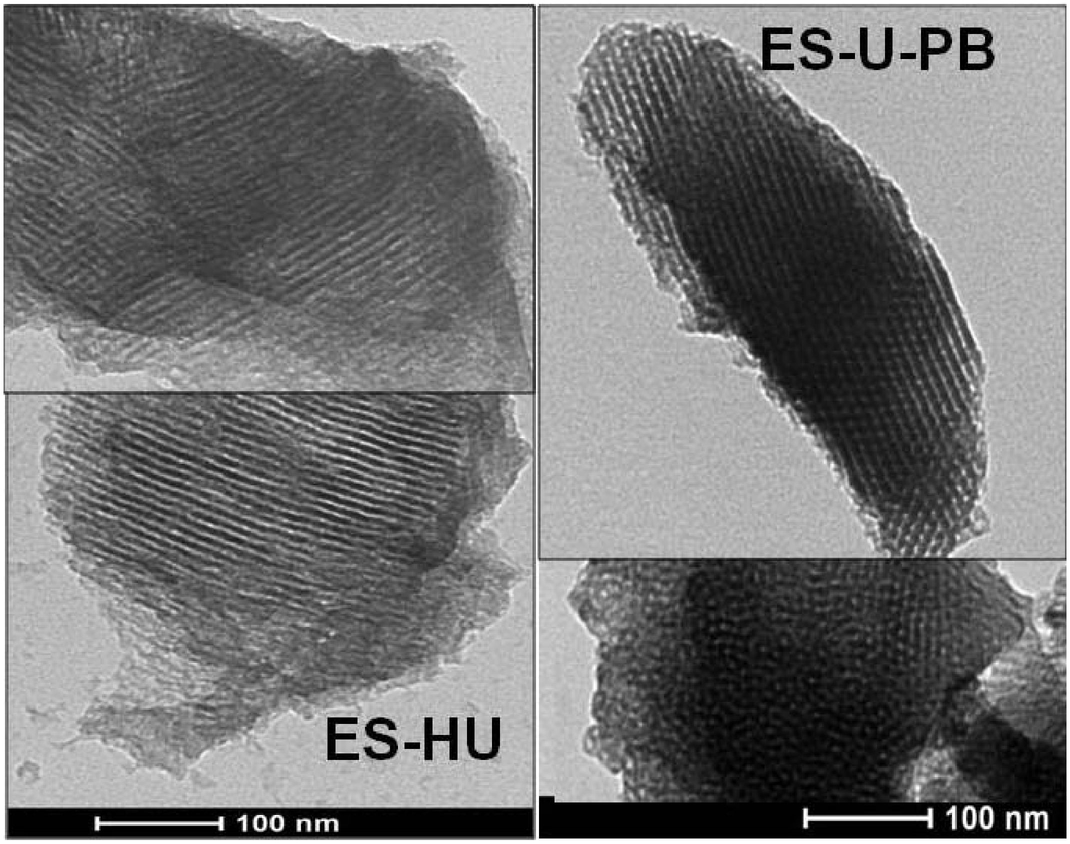

Figure S3. TEM images of the ES-HU and ES-U-PB mesoporous organosilica samples. These images were acquired on a FEI Tecnai G2 Twin microscope (120 kV) at College of Staten Island, CUNY (taken by Dr. Manik Mandal from the group of Professor Michal Kruk); prior to imaging the samples were dispersed in ethanol using sonication and subsequently deposited on a carbon-coated copper grid.

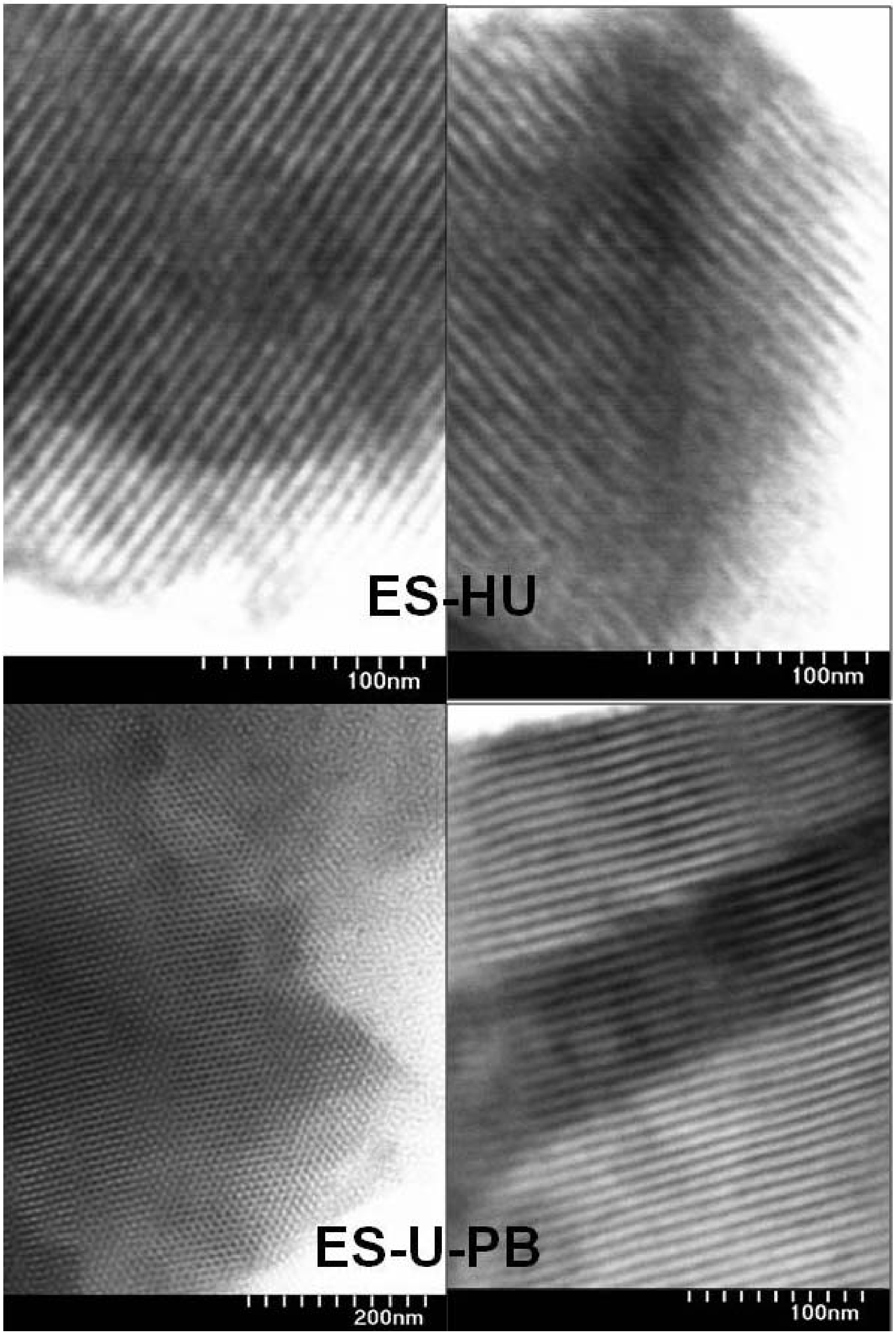

Figure S4. TEM images of the ES-HU and ES-U-PB mesoporous organosilica samples. These images were taken using a Hitachi HD-2000 STEM instrument (200kV) by Drs. P. F. Fulvio and X. Wang at the Center for Nanophase Materials Sciences of the Oak Ridge National Laboratory, which is sponsored by the Division of Scientific User Facilities, US Department of Energy.

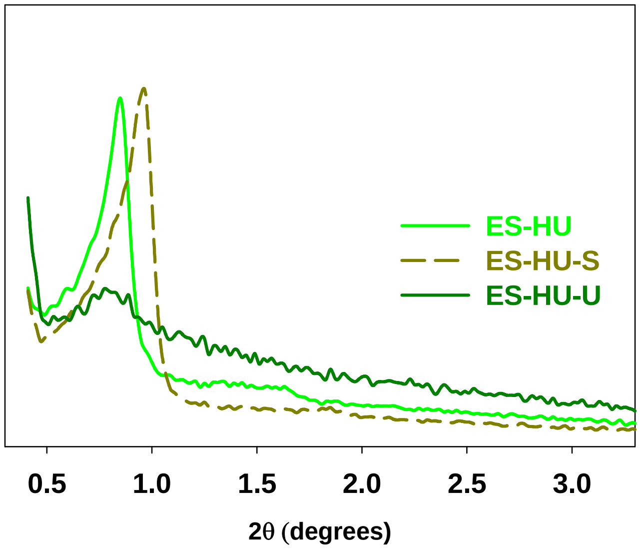

Figure S5. Small angle XRD patterns for the multifunctional PMO samples (ES-HU, ES-HU-S and ES-HU-U) with N-hydroxyurea functionality (formed via reaction of isocyanate and hydroxylamine HCl salt).

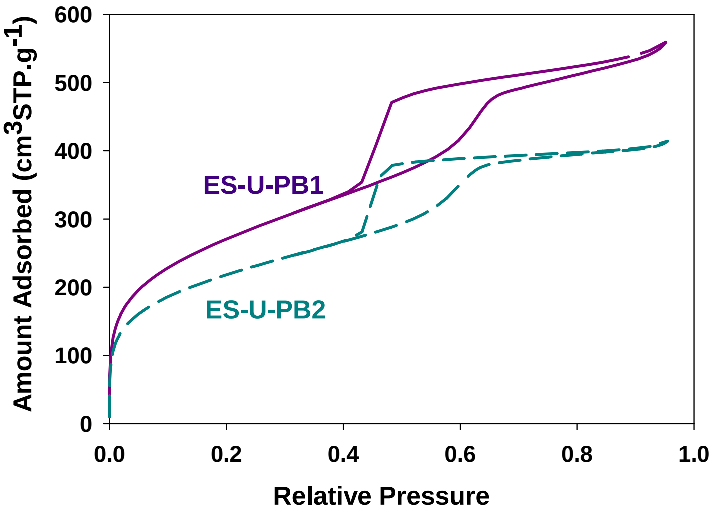

Figure S6. Nitrogen adsorption-desorption isotherms for two ES-U-PB samples having different loadings of reactive precursors.

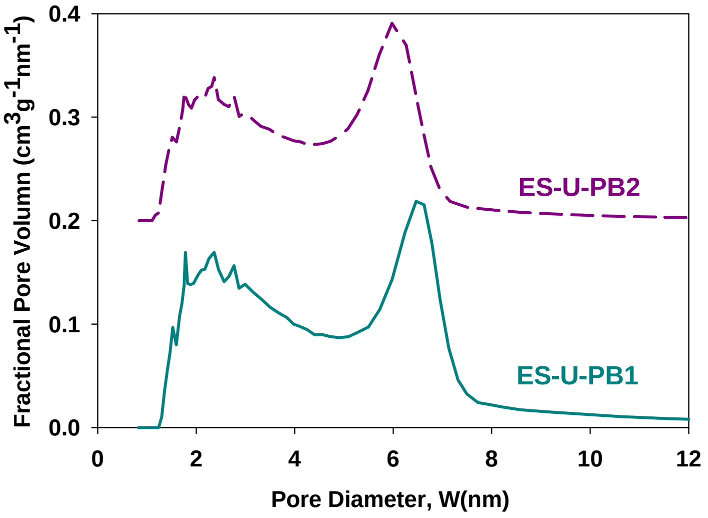

Figure S7. Pore size distributions for two ES-U-PB samples having different loadings of reactive precursors.

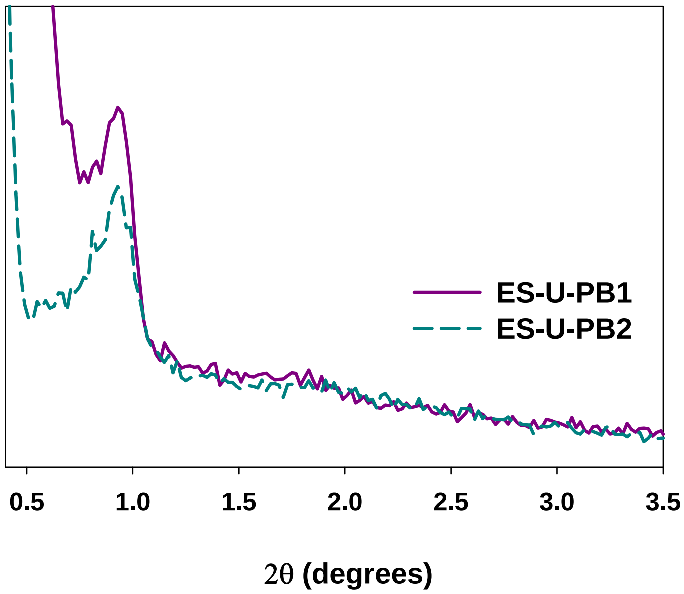

Figure S8. Small angle XRD patterns for two ES-U-PB samples having different loadings of reactive precursors.

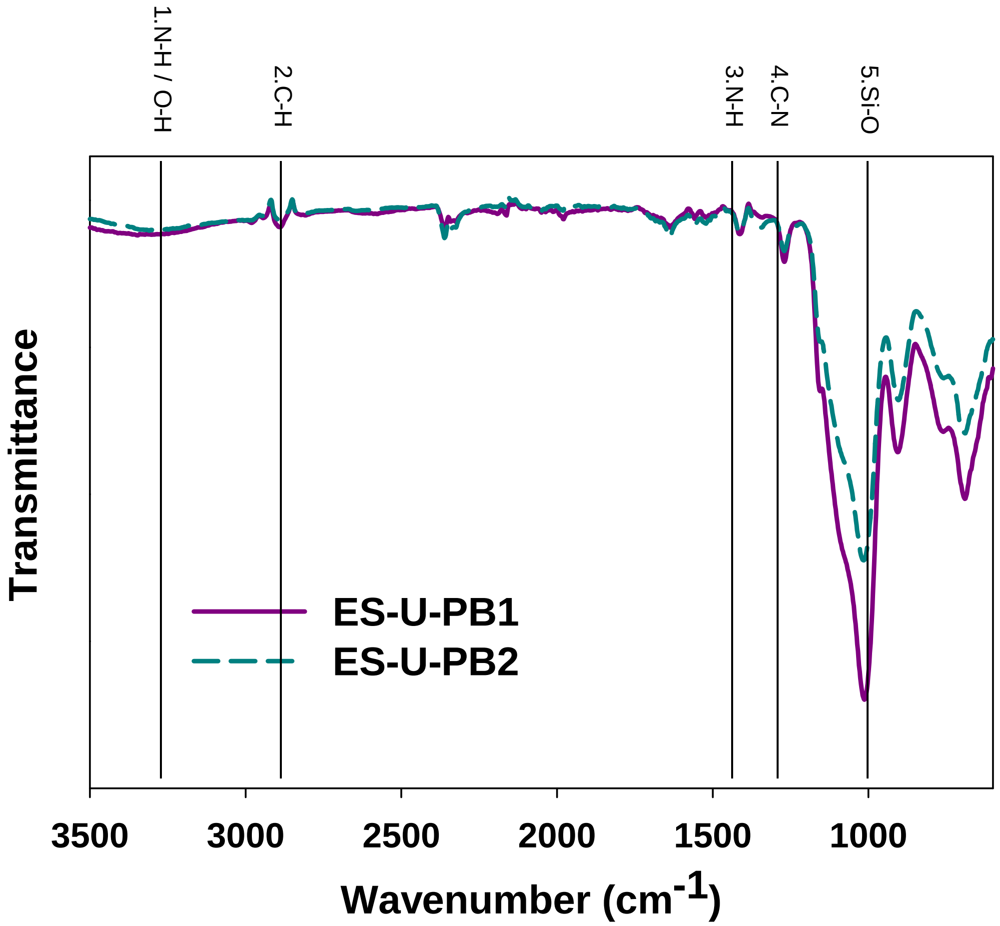

Figure S9. IR patters of two ES-U-PB samples having different loadings of reactive precursors; typical urea peaks are at 1622, 1580, 1530 cm^{-1}. The broad peaks (1) between 3000 and 3500 cm^{-1} can be attributed to N-H stretch and O-H stretch, the peaks (2) around 2900 to 3000 cm^{-1} can be assigned to C-H stretch, the peaks (3) around 1500 cm^{-1} could be caused by N-H stretch and amide II bands, the peaks (4) around 1300 cm^{-1} can be attributed to C-N stretch, and the high intensity peaks (5) below 1110 cm^{-1} are mainly related to Si-O in the ethane-silica framework. The peaks characteristic to organic functionalities are less visible due to high intensity of peaks (5) related to silica.

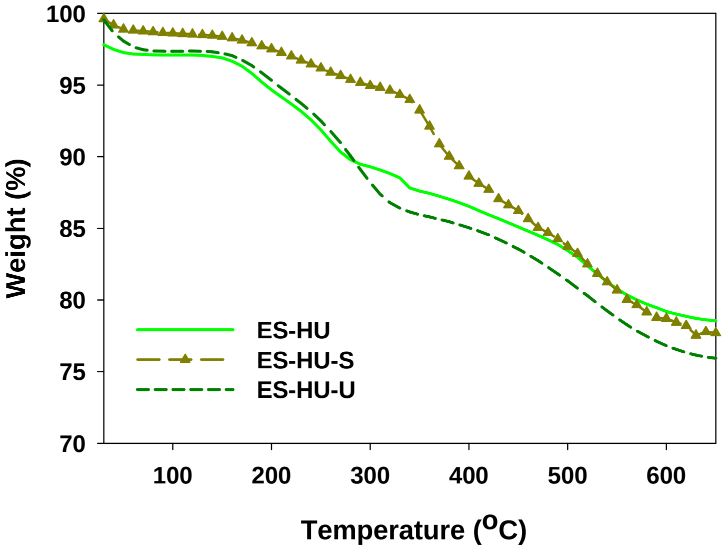

Figure S10. TG weight change profiles for the multifunctional PMO samples (ES-HU, ES-HU-S and ES-HU-U) with N-hydroxyurea functionality (formed via reaction of isocyanate and hydroxylamine HCl salt).

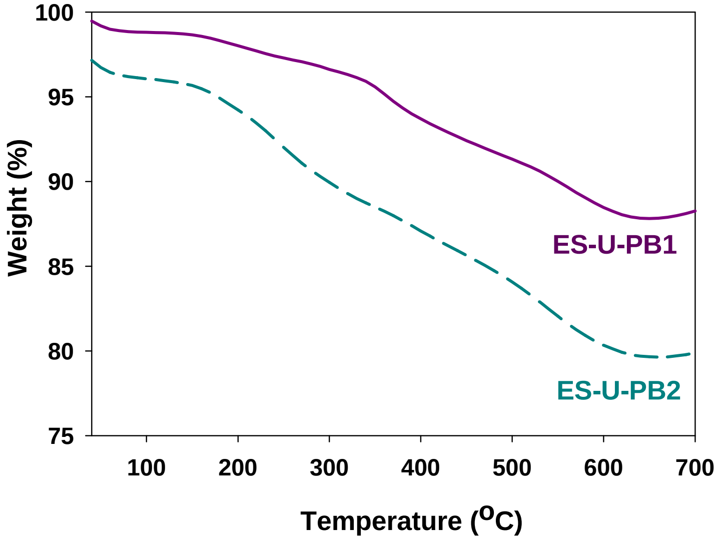

Figure S11. TG weight change profiles for two ES-U-PB samples having different loadings of reactive precursors.

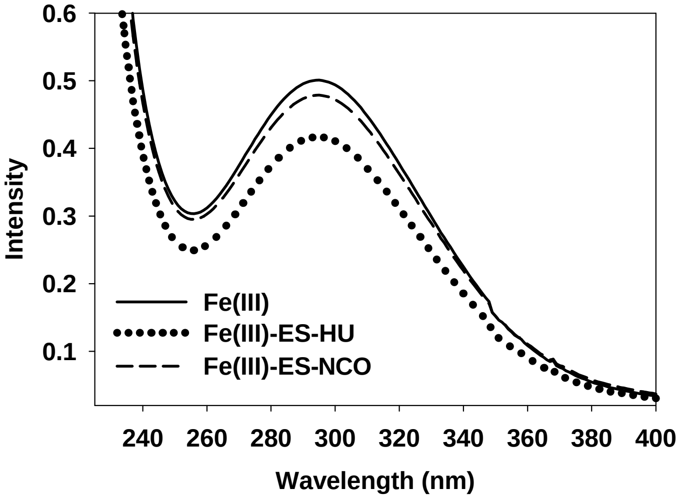

Figure S12. UV-vis spectra of Fe(III)-ES-HU and Fe(III)-ES-NCO systems in comparison to that of Fe(III) solution.

Figure S13. Pictures of Fe(III) chloride solution with ES-HU (3) and ES-NCO (2) samples in comparison to that of Fe(III) chloride solution only(1).